Laser-induced damage of 1064-nm narrow-band interference filters under different laser modes

Weidong Gao (高卫东), Hongbo He (贺洪波), Jianda Shao (邵建达), and Zhengxiu Fan (范正修)

Shanghai Institute of Optics and Fine Mechanics, Chinese Academy of Sciences, Shanghai 201800

Received March 30, 2004

The laser-induced damage behavior of narrow-band interference filters was investigated with a Nd:YAG laser at 1064 nm under single-pulse mode and free-running laser mode. The absorption measurement of such coatings has been performed by surface thermal lensing (STL) technique. The relationship between damage morphology and absorption under the two different laser modes was studied in detail. The explanation was given by the standing-wave distribution theory.

OCIS codes: 310.0310, 310.6870.

Narrow-band interference filters are used to pass radiation in prescribed wavelength band and reject radiation outside of the passband. Its applications are extremely diverse in laser technology and modern optics. However, due to the resonant absorption of interference filters at intense laser radiation, narrow-band interference filters are the components which are vulnerable in the high power laser systems[1], and the laser damage properties of such coatings are significantly different from those of high reflective (HR) coatings and antireflective (AR) coatings. There are little relevant reports on the damage mechanisms of the narrow-band interference filters on optical windows in laser systems[2]. Therefore, it is necessary to investigate the laser damage properties of narrow-band interference filters.

In order to better understand the damage behavior of them, the narrow-band interference filters were designed and deposited as follows, then the laser-induced damage thresholds (LIDTs) of the filters were determined by irradiations with a Nd:YAG laser at 1064 nm under different modes. The filters were deposited on BK7 glasses using VEECO coater. The samples had the same typical construction, A/14(0.81H0.81L) 4(HL) 2H 10(LH) L 2H 4(LH)/G, where G indicated BK7 glass, H stood for high index material Ta_2O_5 with one quarter wavelength optical thickness (QWOT), L stood for low index material SiO_2 with one QWOT, and A was the incident medium, air. The central wavelength of the filters was 1064 nm. The transmission spectra of the samples were measured by a LAMBDA900 spectrometer (see Fig. 1). In the experiment, thin film design software (TFCalc^{TM}) was used in the design and electric field distribution simulation of the filters.

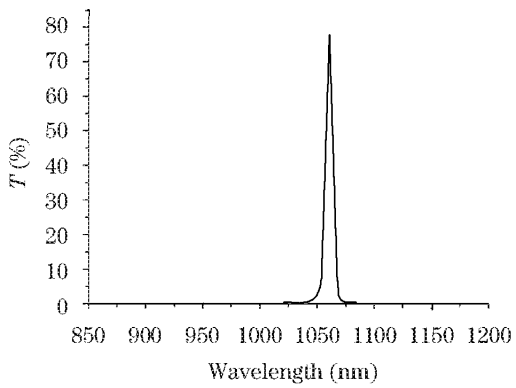

Fig. 1. Measured transmission spectrum of Ta_2O_5/SiO_2 two-cavity narrow-band interference filter.

The calculated standing-wave field distribution of a Ta_2O_5/SiO_2 two-cavity narrow-band interference filter with a high-index-material spacer is shown in Fig. 2. According to Hu's[2] analysis, in the spacer (the resonant cavity of the interference filter) there is a resonant field due to the standing-wave electric field's resonant overlaps. The amplitude is strengthened as the reflectance increases, and, when $R \to 1$, $|\mathbf{E}| \to \infty$. Location of the maximal electric field depends on the refractive index of the spacer. When the spacer layer is made from high-index material (H), the maximal field occurs at both sides of the spacer. When the spacer layer is made from low-index material (L), the location is in the middle of the spacer. In Fig. 2, there are two intense electric field zones and the maximal field occurs at both sides of the spacer, and the electric field is much intense in the spacer near the incidence medium.

The weak absorptance of the filters was measured with surface thermal lensing (STL) technique[3–6]; the absorptance was about 1500 ppm. The high absorptance is mainly attributed to the resonant absorption of interference filters. Though absorptance of material is independent of **E** fields, a high **E** field has more energy for the material to absorb, and thereby the temperature increases in the presence of high **E** fields. As a result, the temperature rise is more significant in the spacer layer

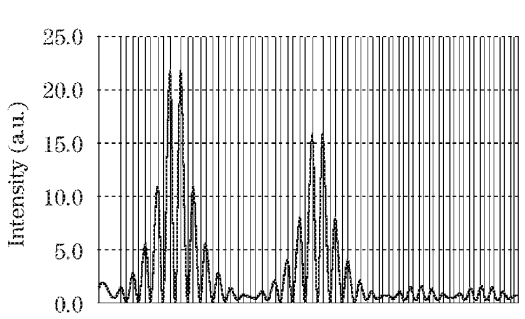

Fig. 2. Standing-wave distribution for the two-cavity narrow-band interference filter with the calculating wavelength of 1064 nm.

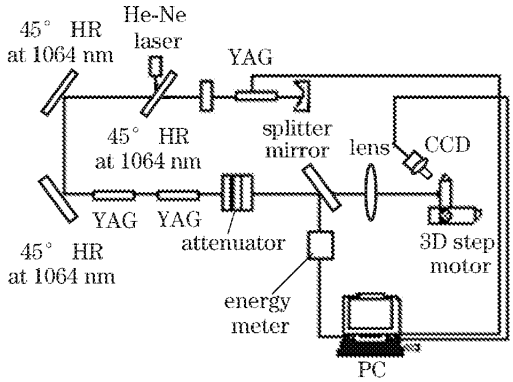

Fig. 3. The measuring instrument of LIDT (1-on-1).

because of the resonant overlap of the standing-wave electric field in the spacer layer. Thermal-stress gradient is induced and initiates the damage of the filter if the irradiation energy reaches to a high level.

The test method of LIDT is 1-on-1, according to the standard ISO/DIS 11254-1.2[7]. A 1064-nm Nd:YAG laser is adopted in the experiment. Figure 3 is the experimental setup. In the case of single-pulse laser mode, the Q-switched laser produces a TEM_{00} mode with a 12-ns pulse width, the size of laser beam is 0.406 mm in diameter. The probe laser is He-Ne laser. Attenuators are used to adjust the pulse energy. In the case of free-running laser mode (free-running laser is also named free-vibration laser), giant pulse of which is the combination of many pulse peaks. In experiment, the total pulse width is 220 μs, the size of laser beam is 0.325 mm in diameter. The LIDT of the filter is 1.9 J/cm^2 for single pulse laser and 35 J/cm^2 for free-running laser.

Figures 4 and 5 show the damage morphology of the filters in the case of single-pulse laser and free-running laser. It is easy to find the difference between the damage morphologies of two laser modes. For single-pulse laser, the damage is evidenced by the removal of top tantalum oxide and silicon dioxide layers and the melting of the layers below them, and the sharp edges indicate the clean, perhaps explosive removal of surface layers. The morphology of the areas within the pitted regions exhibits a structure similar to the material formation produced by intense heating to melting, followed by rapid cooling. The dark spots are areas where the local heating was intense. For free-running laser, microscopic inspection reveals that the typical damage morphology is characterized by a melting of the irradiated area. In Fig. 5, the damage has obvious characteristics: there is a big hole in the center of damage spot with a ring rising, the film is melted and then solidified near the hole by rapid cooling. With the increase of radiation energy density, the hole becomes so deep that the thin film is pierced. Finally, the substrate is fractured in the center of the irradiated spot.

It was shown that narrow-band interference filters had

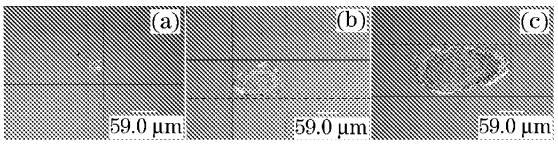

Fig. 4. Optical micrographs of typical damage of narrow-band interference filters with single pulse laser after a single shot under different energy densities. (a): 4.1 J/cm^2; (b): 6.5 J/cm^2; (c): 10.3 J/cm^2.

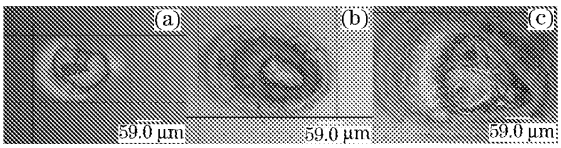

Fig. 5. Optical micrographs of typical damage of narrow-band interference filters with free-running laser after a single shot under different energy densities. (a): 98.9 J/cm^2; (b): 154.4 J/cm^2; (c): 247.6 J/cm^2.

unique laser-induced damage behavior. The reinforced resonant field in the spacer layer induced an increase in the absorptance and a decrease in the LIDT. Hu[2] and Ctaguro[1] thought the damage initiated in the spacer of the filters, which agreed with our conclusion. However, in our experiment, there was an obvious difference between the damage morphologies of the two laser modes, which was probably attributed to the different behaviors of the two laser modes. In the case of single-pulse laser, because of the high peak power of single pulse laser, laser-induced thermal-stress coupling would play the key role in the damage of the filters. But in the case of free-running laser, the heat deposition became the leading factor in the damage of the filters for the laser's lower power and accumulation effect. Further work is in progress.

This work was supported by the National "863" Project of China. W. Gao's e-mail address is wdgao@mail.siom.ac.cn.

References

1. W. S. Ctaguro, Proc. SPIE **414,** 36 (1974).
2. H. Y. Hu, Z. X. Fan, and F. Luo, Appl. Opt. **40,** 1950 (2001).
3. Z. L. Wu, P. K. Kuo, and Z. X. Fan, Proc. SPIE **2428,** 113 (1995).
4. Y. J. Wang, J. Wang, Q. G. Li, and Z. X. Fan, Chin. J. Lasers **28,** 765 (2001).
5. D. W. Zhang, S. H. Fan, and W. D. Gao, Chin. Opt. Lett. **2,** 305 (2004).
6. J. P. Hu, P. Ma, and Q. Xu, Chin. Opt. Lett. **1,** 340 (2003).
7. Optics and optical instruments – Lasers and laser related equipment – Test methods for laser induced damage threshold of optical surfaces – Part 1: 1 on 1 test, ISO/DIS 11254-1.2.